Materials Science & Engineering A 731 (2018) 161–172

Contents lists available at ScienceDirect

Materials Science & Engineering A

journal homepage: www.elsevier.com/locate/msea

Creep strength and minimum strain rate estimation from Small Punch Creep tests

S. Holmström[a,*], Y. Li[b], P. Dymacek[c], E. Vacchieri[d], S.P. Jeffs[e], R.J. Lancaster[e], D. Omacht[f], Z. Kubon[f], E. Anelli[g], J. Rantala[h], A. Tonti[i], S. Komazaki[j], Naveena[j], M. Bruchhausen[a], R.C. Hurst[e], P. Hähner[a], M. Richardson[k], D. Andres[l]

[a] European Commission, JRC, Petten, The Netherlands
[b] Retired from DNV-GL (KEMA), The Netherlands
[c] Institute of Physics of Materials, Brno, Czech Republic
[d] Ansaldo Energia S.p.A, Genova, Italy
[e] Swansea University, Swansea, UK
[f] MMV, Brno, Czech Republic
[g] Franchini Acciai S.p.A, Mairano, Italy
[h] VTT Technical Research Centre LTD, Espoo, Finland
[i] INAIL, Rome, Italy
[j] Kagoshima University, Kagoshima, Japan
[k] United Kingdom Atomic Energy Authority (UKAEA), UK
[l] Universidad de Cantabria, Santander, Spain

ARTICLE INFO

Keywords:
Small Punch Creep test
SPC
Creep strength
Creep strain rate
Standardization

ABSTRACT

A new standard is currently being developed under the auspices of ECISS/TC 101 WG1 for the small punch testing technique for the estimation of both tensile and creep properties. Annex G of the new standard is covering the assessment and evaluation of small punch creep (SPC) data. The main challenge for estimating uniaxial creep properties from SPC data is the force to equivalent stress conversion between SPC and uniaxial creep tests. In this work a range of SPC assessment methodologies, benchmarked for the standard, are compared for verifying the best practice used in the standard. The estimated equivalent stresses for SPC are compared to uniaxial creep stresses at equal rupture times, using three alternative models. In-depth analyses are performed on SPC and uniaxial creep data for P92, F92 and 316 L steel tested within an inter-laboratory round robin. The formulation for SPC equivalent creep strain rate in the standard is also assessed.

1. Introduction

The small punch creep (SPC) test is a miniature technique where a hemispherical ended puncher (or a ceramic ball) deforms a thin metal disc, as a function of time, at constant temperature and force until rupture occurs. The most used type of SPC specimen is the 0.5 mm thick disc with a diameter of 8 mm [1]. The SPC test has found many uses, e.g. the SPC test is especially suitable for material creep property estimation when material is scarce and a standard type specimen cannot be manufactured, e.g. characterizing heat affected zones in welds [2–4]. The methodology is virtually non-invasive when applied on in-service thick section components [5]. The method can also be used as a ranking method for novel materials manufactured in very small quantities [6]. However, the many challenges in SPC test data interpretation [7] have hindered the methodology to find wider use. The currently ongoing standardization work on small punch testing is envisaged to remedy this.

The SPC test is one of two test types to be standardized in a new EN standard due to be published 2019. The standard also covers the use of SP for fracture mechanical properties estimations. The small punch testing standard is prepared within the European Committee for Iron and Steel Standardization (ECISS), Technical Committee 101 (TC101), working group 1 (WG1). The standard covers the classical Small Punch (SP) test for tensile property estimation [8,9] and the Small Punch Creep (SPC) test for creep property evaluation [10]. The assessment methodologies tested for finding a best practice for estimating creep properties by SPC are presented in this paper together with test data produced within WG1 in support of the standard.

* Corresponding author.
E-mail address: Stefan.holmstrom@ec.europa.eu (S. Holmström).

https://doi.org/10.1016/j.msea.2018.06.005
Received 9 April 2018; Received in revised form 1 June 2018; Accepted 2 June 2018
Available online 04 June 2018

To successfully be able to estimate "uniaxial" creep properties by SPC testing, which is in nature a biaxial test, a robust method to convert the applied SPC force to an “equivalent” stress has to be established. The basis of this conversion is that the equivalent SPC stress and the uniaxial creep stress give equal test durations. This task has been shown to be challenging. The classical formulation described in the code of practice CWA 15267 [1], has been used as a basis for the assessments presented in this paper but has shown to be insufficient to account for apparent temperature and load dependency in the conversion of SPC load to equivalent stress [11]. When uniaxial creep data is available the conversion factor can be optimized by direct correlation but if no such data is available the factor has to be applied without "ductility" correction. A number of methods have been proposed to remedy the shortcomings of the classical approach by introducing different correction factors [12–15].

New insight in the assessment of classical small punch (SP) for determining dynamic tensile properties and SPC data has shown that the main contributor to the temperature and force dependency in the conversion from force to stress is in fact a deflection (or displacement) dependency, i.e. related to the effective contact area under the punch. In this paper two new assessment approaches, with improved conversion accuracy of SPC equivalent stress, are benchmarked against the classical methodology with a constant conversion factor. The two other models are also benchmarked "as-is" without further correction to the available uniaxial creep data. To validate the model robustness in prediction the acquired SPC equivalent stresses are plotted against the corresponding (same rupture time) uniaxial creep stress.

In the draft standard the parameters for force to stress conversion and the conversion between minimum deflection rate and minimum creep strain rate is given for one SPC test configuration, i.e. for a clamped 0.5 mm thick specimen punched by a ∅2.5 mm puncher (or ball) into a ∅4 mm receiving hole. The receiving hole can either have a chamfer (0.2 mm deep ∠45°) or a radius (0.2 mm).

An example of a standard test assembly is shown Fig. 1.

To support the standardization of the SPC tests the TC101 working group, institutions listed in Table 1, have generated data in an inter-laboratory testing campaign [7]. These data are published and analysed in this paper.

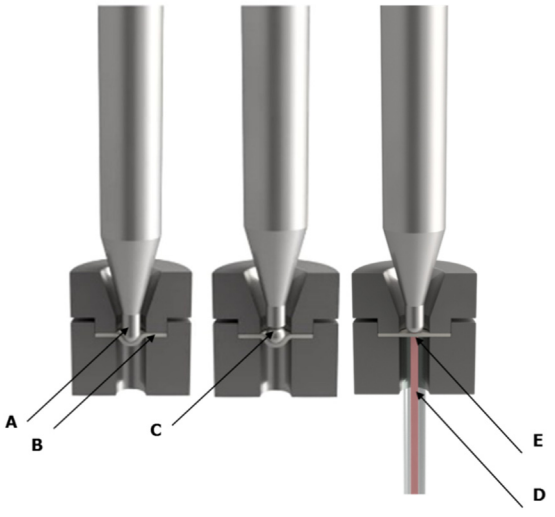

Fig. 1. Small punch test set-up with puncher (A) or ball (C). The specimen (B) is clamped to avoid upward bending of the specimen. The displacement is measured from below, e.g. through the movement of a ceramic rod (D). The temperature is measured from a thermocouple (E) integrated in the rod or in the clamping tool close or touching the specimen.

Table 1
Organizations that have provided test material (MP), generated uniaxial creep data (UA) and/or small punch creep data (SPC) in support of the standard.

Organization	Abbreviation	Country	Data
Institute of Physics of Materials	IPM	Czech Republic	SPC
Material & Metallurgical Research, Ltd.	MMV	Czech Republic	SPC, UA, MP
European Commission – JRC	JRC	The Netherlands	SPC, UA, MP
Swansea University	SWA	United Kingdom	SPC
Ansaldo Energia S.p.A.	ASEN	Italy	SPC
VTT Technical Research Centre of Finland LTD	VTT	Finland	SPC
United Kingdom Atomic Energy Authority	UKAEA	United Kingdom	SPC
INAIL	INAIL	Italy	SPC
Franchini Acciai S.p.A.	FRA	Italy	UA, MP
Kagoshima University	KAG	Japan	SPC

2. Materials

The TC101-RR test programme for supporting the SPC part of the small punch standard (named after the technical committee) includes uniaxial creep and SPC testing on two variants of the ferritic/martensitic grade 92 steels, i.e. one P92 pipe and one large forging F92. In addition a single variant of an austenitic steel 316 L has been tested. The room temperature proof strength (R_{p02}) and the ultimate tensile strength (R_m) for the tested steels are given in Table 2 together with some information on product form, heat treatments and availability of uniaxial creep data. Note that the reference uniaxial creep data sets are generally limited and the test durations covered are short.

The table clearly emphasizes the different proof strengths. A lower proof strength, as for the 316 steel, will impact the initial plastic deformation, deflection expected after loading and the level of local strain hardening at the beginning of the SPC test.

3. Models and methods

To be able to compare the creep strengths of the uniaxial data against the estimated strengths from SPC tests, the uniaxial stress at specific times to rupture periods needs to be determined. For this purpose, the uniaxial creep rupture data has been modelled to facilitate interpolation (or extrapolation) of the uniaxial creep strength properties.

The models presented for converting force to equivalent stress from SPC data look to establish a constant or deflection dependent force to stress ratio $\Psi = F/\sigma$. When plotting the calculated equivalent stresses from SPC data against the corresponding uniaxial creep strengths with the same rupture time ($t_{r\text{-}UA} = t_{r\text{-}SPC}$), they should optimally fall on the 1:1 unity line. Another consideration would naturally be to compare stress versus time to rupture plots. However the stress comparison route was chosen to accommodate the confidentiality of some of the uniaxial creep test results. Note that both the uniaxial (interpolated) stress and the equivalent SPC stress thus depend on the SPC test results, i.e. the SPC time to rupture will affect the determined corresponding uniaxial creep stress and the deflection at minimum deflection rate will affect the SPC equivalent stress. For instance if a SPC test ruptures prematurely (decrease in t_r) the corresponding (interpolated) uniaxial creep stress will increase and if the deflection at minimum deflection rate is reduced the equivalent SPC stress will increase.

3.1. Uniaxial reference data, creep rupture and minimum strain rate models

The uniaxial creep test programmes performed for the TC101-RR are presented in Tables 3 and 4. The short term uniaxial data made available for the SPC assessment for F92 steel consists of six tests, four data points at 600 °C and two at 625 °C.

Table 2
TC101-RR test materials and heat specific proof strength (R_{p02}) and ultimate tensile strength tensile strength (R_m).

Material	Source	Product form	Heat treatment	R_{p02} (RT) MPa	R_m (RT) MPa	Uniaxial creep data
P92	MMV	Pipe, ø219.1 × 22.2 mm	Normalized and tempered	594	753[a]	Available
				679	808[b]	
				720	860[c]	
F92	FRA	Forging (thick)	Normalized and tempered	470	645	Assessor only[d]
316 L (1.4404)	JRC	Plate (thick)	Annealed	235	569	Available

[a] Material certificate.
[b] MMV test (hoop direction).
[c] JRC test (axial direction).
[d] The uniaxial time to rupture data for the F92 steel is confidential within ECCC.

Table 3
Isotherms, number of tests and uniaxial creep rupture stress levels for the P92 tube as reported by MMV and JRC. The longest test duration to rupture is 5803 h and the shortest is 3.4 h.

Isotherm (°C)	Nr. of data points	Stress range (MPa)
600	6	190–240
625	10	125–250
650	10	110–220
Total	26	110–250

Table 4
Isotherms, number of tests and uniaxial creep rupture stress levels for the 316 L plate as reported by JRC. The longest test duration to rupture is 593 h and the shortest 0.4 h.

Isotherm (°C)	Nr. of data points	Stress range (MPa)
650	5	160–220
675	1	170
700	6	120–240
Total	12	110–250

Two models have been used for describing the creep rupture behaviour of the uniaxial tests, i.e. the Wilshire model (WE) [16] and a log-linear Larson-Miller (LM) [17] model. The log-linear LM model is clearly the simplest approach for comparison and is defined in Eqs. (1) and (2) for P92 and 316 L respectively. The Larson-Miller parameter is defined in Eq. (3). The constants, C, for P92 and 316 L are $C = 32$ and $C = 24$ respectively.

P92:

$$\log(\sigma) = 6.3494 - 0.132 \cdot P_{LM} \quad (1)$$

316 L:

$$\log(\sigma) = 4.2887 - 0.1063 \cdot P_{LM} \quad (2)$$

The Larson-Miller time-temperature parameter P_{LM} is defined in Eq. (3);

$$P_{LM} = \frac{(\log(t_r) + C) \bullet (T+273)}{1000} \quad (3)$$

where the temperature T is given in Celsius (°C) and t_r is the measured time to rupture in hours (h). The constant C of the P_{LM} is optimized and defined for each test material. The stress against P_{LM} plots for P92 pipe and 316 L plate are given in Fig. 2.

To describe the "goodness of fit" the measured stress is plotted against the predicted stress as shown in Fig. 3. This plot type is an ECCC post assessment test plot [18] which is used to describe how well the model performs. The acquired confidence bands for stress, here 2.5·standard deviations, are used as a base for the SPC assessments later in this paper. The larger scatter bands found for P92 uniaxial data is likely to be caused by the test being performed in two testing laboratories and also different sample extraction direction between the labs. The JRC test samples were extracted in the axial direction and MMV tests were extracted perpendicularly to the axis over the wall thickness of the pipe.

The more complex Wilshire model (WE) as described in Eq. (4) was used for the P92 and F92 steels since it was found that the LM model overestimated the creep stress in backwards extrapolation, i.e. in the short time range for these steels.

The WE model has the advantage of having an analytical equation for both time to rupture and stress at rupture. Also, the data is fitted in normalized stress limiting the stress below a specified reference stress, e.g. the ultimate tensile strength R_m.

The predicted creep rupture strength σ for a specified time to rupture t_r using the Wilshire model is defined as:

$$\sigma = \exp(-k(t_r \cdot \exp(\frac{-Q}{R \cdot T}))^u) \cdot R_m(T) \quad (4)$$

where $R_m(T)$ is the ultimate tensile strength at test temperature, Q the apparent creep rupture activation energy, R the gas constant and k and u are fitting parameters.

The tensile strength data as a function of temperature for the P92 (TC101) heat, used for normalizing in Eq. (4), is publicly available in the JRC data base [19]. For the 316 L steel the tensile strength for the particular batch was not available and the normalization was achieved by using the 316 strength by Schirra et al. [20]. It was found that the LM model worked well for 316 L also in extrapolations towards shorter test durations. Thus, the following SPC data assessments use the Larson-Miller approach for 316 L and the Wilshire model for P92 and F92.

A small data set of uniaxial creep tests was provided for F92 by the ECCC work group 3 A for confidential assessment. The F92 uniaxial data was assessed with the same procedure as for P92 using the same tensile strengths for normalizing. The normalization of the WE model with higher strength tensile values might affect predicted stresses for extrapolated short term tests, i.e. close to the tensile strength. This is also the case for extrapolations toward shorter test durations with the LM model.

To describe the creep minimum strain rate behaviour of the uniaxial creep tests, the Monkman-Grant (MG) [21] relationship has been used. The MG approach correlates time to rupture and the minimum creep $\dot{\varepsilon}_c$ rate as:

$$t_r = \frac{B}{\dot{\varepsilon}_c^m}(\mathrm{h}) \quad (5)$$

where B and m are material dependent constants. Using the MG relationship, the SPC tests can be assessed for correlation between the measured minimum deflection rate and the uniaxial minimum strain rate at equal t_r as described later in this paper. The B and m for P92 and 316 L are given in Table 5. Note that the minimum strain rate for 316 L at equal time to rupture is roughly five times higher than for P92.

The MG predicted strain rate versus the measured strain rates are shown for the few tests with strain measurement for P92 and 316 L in Fig. 5.

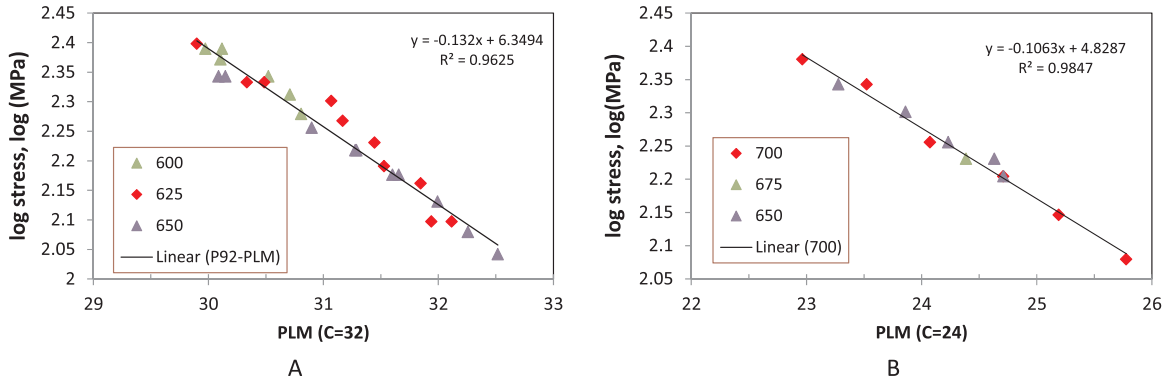

Fig. 2. Uniaxial creep data P_{LM}-stress plot defining Eq. (1) for a) P92 pipe and Eq. (2) for b) 316 L plate using Eq. (2).

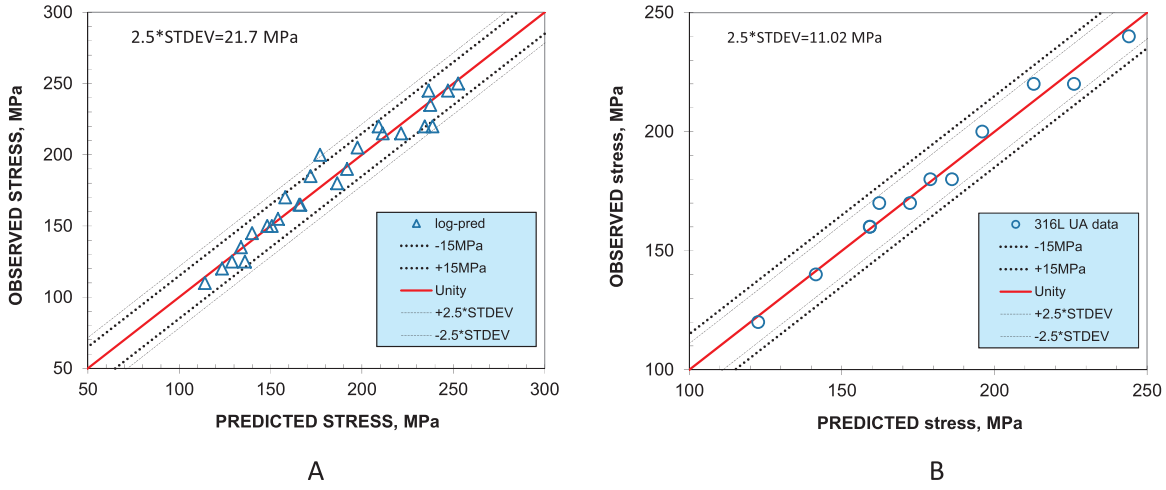

Fig. 3. Observed uniaxial stress against predicted uniaxial stress for a) P92 and b) 316 L plate using the Larson-Miller models (Eqs. (1) and (2)).

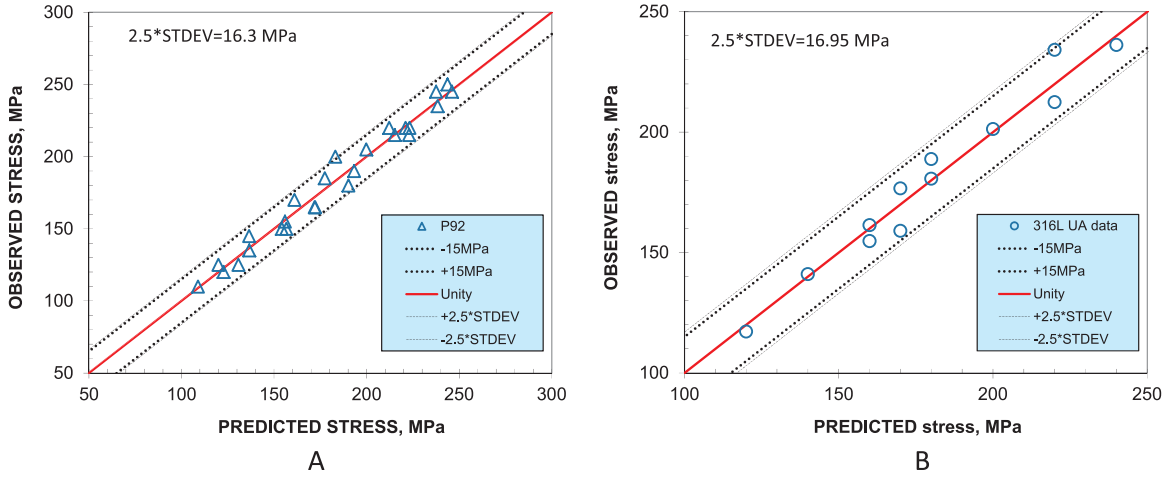

Fig. 4. Observed uniaxial stress against predicted uniaxial stress for a) P92 pipe and b) 316 L plate using the WE model.

Table 5
Monkman-Grant material parameters for P92 and 316 L.

Material	B	M
P92	0.0443	0.9443
316 L	0.2313	0.9909

3.2. SPC data and force to stress conversion models

The SPC test programmes performed for the TC101-RR are given in Tables 6–8.

In a number of the P92 SPC tests, unexpected changes in the deflection rate were observed during the experiment (see Fig. 6b). To investigate the source of the abnormal curves one of the test conditions

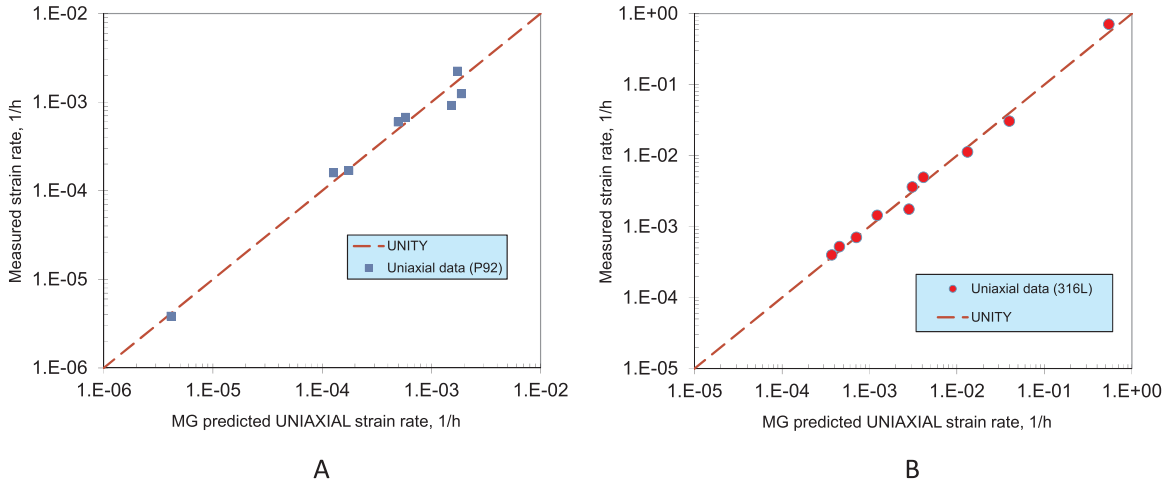

Fig. 5. Measured minimum strain rate against MG predicted minimum strain rate for a) P92 and b) 316 L.

Table 6
Number of tests at specified temperatures and SPC force levels for P92 as reported by SWA, MMV, IPM, KAG, VTT and JRC. The longest test duration to rupture is 521 h and the shortest is 17.8 h.

F [N]	250	275	300	325	350	375	400	425	450	475	500	525	550	Total
600 °C							1		2	**4**	3	3	4	17
625 °C				1	4	**7**	5	4	3					22
650 °C	1	5	5	**7**	5	8								31
Total	**1**	**5**	**5**	**8**	**7**	**15**	**6**	**4**	**5**	**4**	**3**	**3**	**4**	**70**

Table 7
Number of tests at specified temperatures and SPC force levels for F92 forging as reported by ASEN, UKAEA, IPM and JRC. The test programme is still ongoing. The longest test duration to rupture is 562.4 h and the shortest is 2.6 h.

F [N]	300	350	400	450	500	550	600	Total
600 °C			1	2	3	4	2	12
650 °C	1	2						3
Total	**1**	**2**	**1**	**2**	**3**	**4**	**2**	**15**

Table 8
Number of tests at specified temperatures and SPC force levels for the 316 L plate as reported by IPM, ASEN and JRC. The test programme is still ongoing. The longest test duration to rupture is 1658 h and the shortest is 3.1 h.

F [N]	350	390	400	440	450	500	550	Total
650 °C	1		1		1			3
700 °C	1	1	2	1	4	3	1	13
Total	**2**	**1**	**3**	**1**	**5**	**3**	**1**	**16**

was re-tested and interrupted after the abnormal increase in the deflection rate was observed. It was found that the specimen had developed a circumferential crack with a diameter of approximately 1 mm (see Fig. 6a). Premature cracking is likely to reduce time to rupture and potentially also the location in the deflection-time curve where the minimum deflection rate is reached. This will have an impact on both the predicted uniaxial creep stresses and the estimated SPC equivalent stresses. The change in deflection rate, fitted in logarithmic form, can be used as an indicator of premature cracking. In Fig. 7 the polynomial fits to the deflection rate data of the full tests in Fig. 6 show double minima in the deflection rate. These double minima are characteristic for tests with premature cracking.

The P92 tests that did not show anomalies in the time –deflection curve, e.g. the higher temperature tests at 650 °C (see Fig. 8) showed ductile type fractures with some minor radial cracking on the final punch-through neck.

The F92 forging is clearly a softer material than the P92. The lower proof strength is recognized by an increased deflection at loading by F92 in comparison to the P92 samples at equal test force. The uniaxial creep properties are also lower, indicated by lower SPC equivalent stresses at equal test durations. For F92 there was no sign of premature cracking in the deflection-time plots and the post examination of the samples show plastic collapse type failures (see Fig. 9). The evidently extensive oxidation indicates that the protective Argon gas flow had not been sufficient. The impact of oxidation on the time to rupture has not been taken into account in the assessments.

The austenitic stainless steel 316 L (Fig. 10) is again clearly different from the aforementioned P92 and F92 steels. The 316 L steel has an even lower proof strength, resulting in large deflections at loading. Also, the magnitude of strain hardening is expected to be large. The 316 L test curves and post-test examinations showed no sign of premature cracking. The fracture type indicates purely plastic collapse.

3.3. SPC conversion methodologies

Three models for calculating an equivalent creep stress for SPC tests are benchmarked in this paper, i.e. the classical CEN Work Shop Agreement model (CWA model) [1], with a constant force to stress ratio $\Psi = F/\sigma$, a modification of the CWA model with deflection dependency based on the Chakrabarty membrane stretching theory [22] and the empirically defined model incorporated in the new small punch standard.

3.3.1. Classical CWA model

The CEN Work Shop Agreement that precedes the standard defines a test-setup and "ductility" dependent conversion factor between force and stress. The force to stress ratio $\Psi = F/\sigma$ (see Eq. (6)) is based on the Chakrabarty membrane stretching equations. The CWA equation

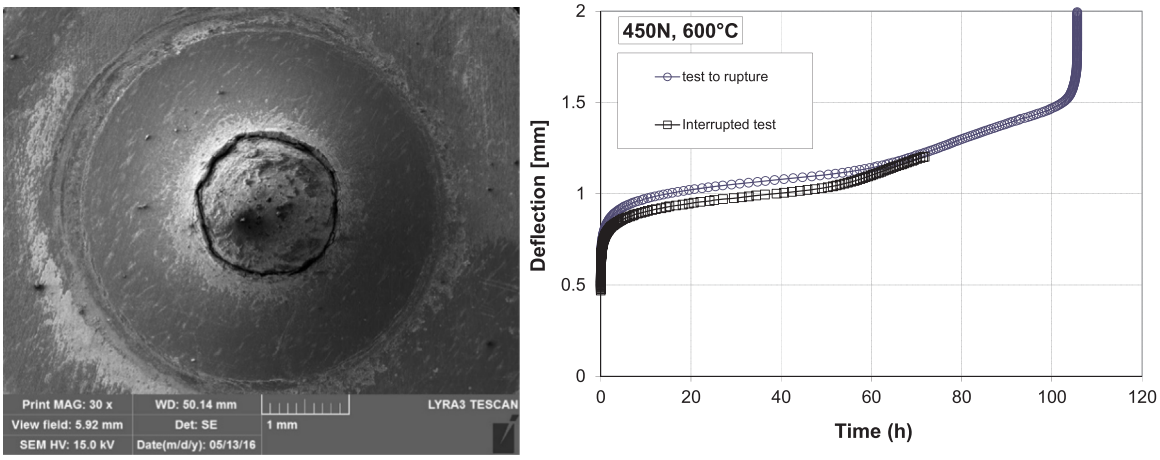

Fig. 6. a) SEM image of an interrupted P92 SPC test sample. The test was interrupted at approximately 70% of time to rupture (test at 600 °C/450 N) as seen in b) the corresponding time deflection curves.

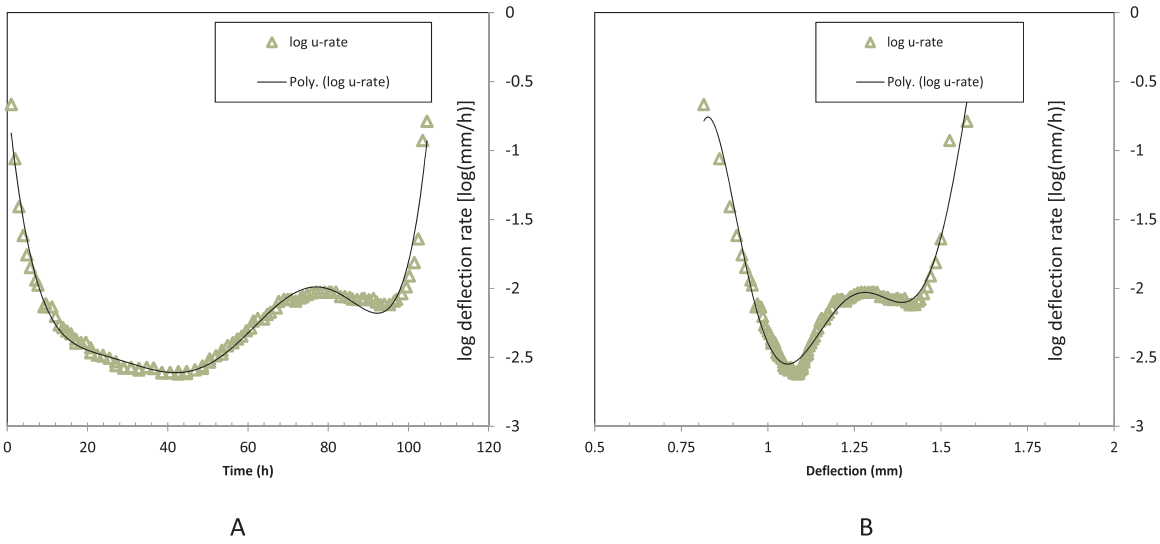

Fig. 7. Polynomial fits of a) time-logarithmic deflection rate and b) deflection-logarithmic deflection rate can be used as an indicator for premature cracking.

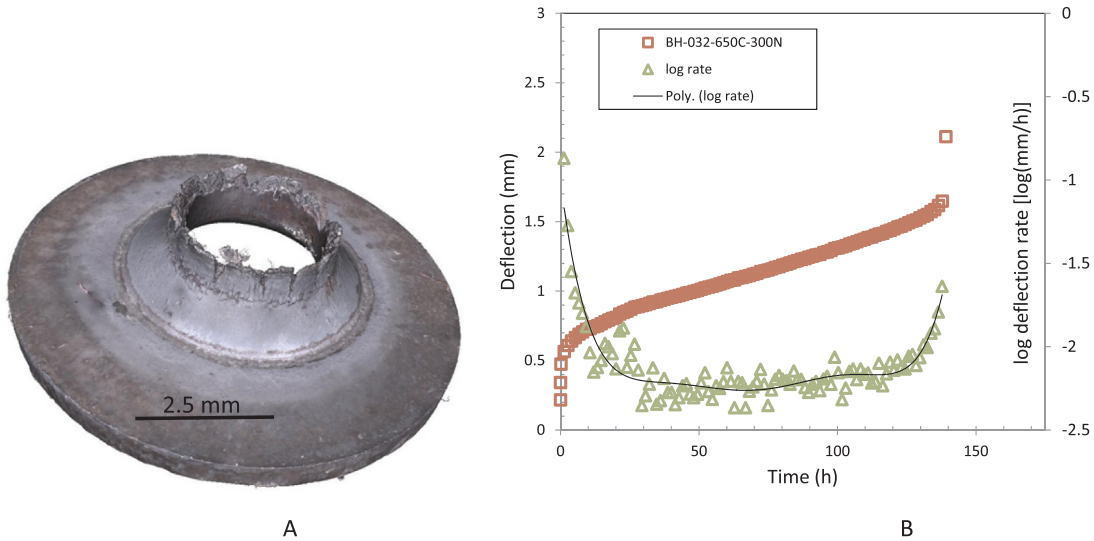

Fig. 8. a) 3D profilometer image of P92 SPC fracture (test BH-032 at 650 °C / 300 N, t_r = 139 h and b) the corresponding time-deflection and deflection rate curves.

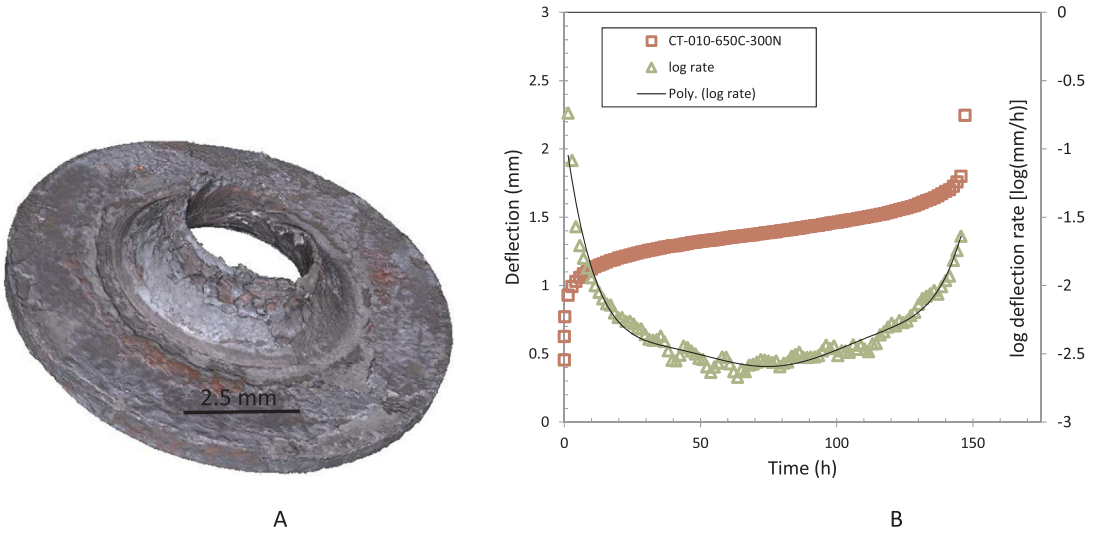

Fig. 9. a) 3D profilometer image of F92 SPC fracture (test CT-010 at 650 °C / 300 N, t_r = 147 h and b) the corresponding time-deflection and deflection rate curves. Note extensive oxidation despite testing in Argon.

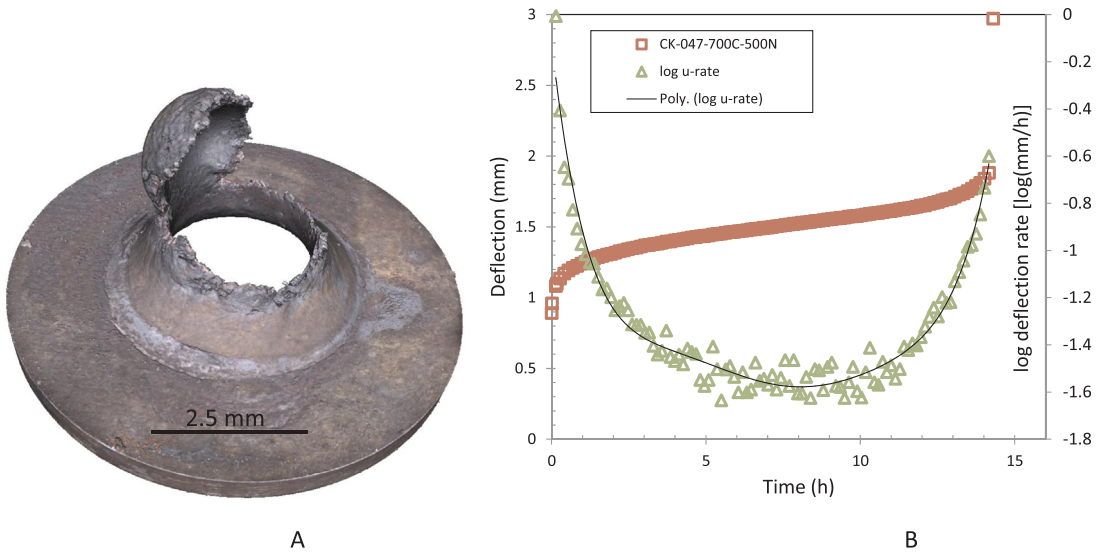

Fig. 10. a) 3D profilometer image of 316 L SPC fracture (test CK-047 at 700 °C / 500 N, t_r = 14.3 h and b) the corresponding time-deflection and deflection rate curves. Note ductile "hat" type fracture.

defines the maximum value of Ψ over the Chakrabarty defined Ψ_{Cha} (u) for differing puncher diameter, receiving hole diameter and specimen thickness. For the standard test set-up this corresponds to a constant value Ψ = 1.895 N/MPa (when k_{SP} = 1). The main benefit of the equation is that it can be applied to different test set-ups.

The CWA force to stress ratio $\Psi_{CWA} = F/\sigma$ is:

$$\Psi_{CWA} = 3.33 \bullet k_{SP} \bullet R^{-0.2} \bullet r^{1.2} \bullet h_0 \,[\mathrm{N/MPa}] \quad (6)$$

where R is the radius of the receiving hole, r is the radius of the puncher or ceramic ball, h_0 is the specimen thickness and k_{SP} is the non-dimensional SPC "ductility" parameter. The k_{SP} is a material specific "ductility parameter" or in reality a tweaking factor that can be applied to correct the Ψ according to uniaxial creep tests. The default value is k_{SP} = 1, originally optimized for P91 steel. It has been shown that the material specific k_{SP} can be both temperature and force dependent [11]. Good correlations can of course be obtained for SPC versus uniaxial creep data when the k_{SP} is optimized against uniaxial data but when no uniaxial data exist, the credibility of the predicted stress is limited. In fact this is the main draw-back of the method and one of the main reasons why SPC testing has not found wider use.

It is to be noted that the original data fit for the CWA model was undertaken on Ferritic-Martensitic steel P91, a steel with very much the same behaviour as the P92 material assessed here. Thus, the model is expected to be in rather good agreement with the P92 SPC tests, possibly also for F92 tests but not likely to work well with 316 L data. The calculated equivalent SPC creep stresses using the CWA model with k_{SP} = 1 are shown against the (interpolated) uniaxial creep stresses at equal creep rupture time in Figs. 11–13 for P92, F92 and 316 L respectively. The scatter bands in the plots are from the preferred uniaxial creep models (± 2.5 STDEV), i.e. as in Fig. 4a) for P92. It can be seen that the original CWA model is indeed predicting well for the P92, though the creep stresses are slightly under predicted (~5%) by the SPC data. The scatter in the vertical direction of each level of SPC equivalent stress is caused by the temperature and load dependency of the k_{SP}. The calculated equivalent stresses for both F92 and 316 L are clearly overestimated. The over estimation is a result of the force and temperature dependence of k_{SP} for the more ductile materials with a lower proof strength.

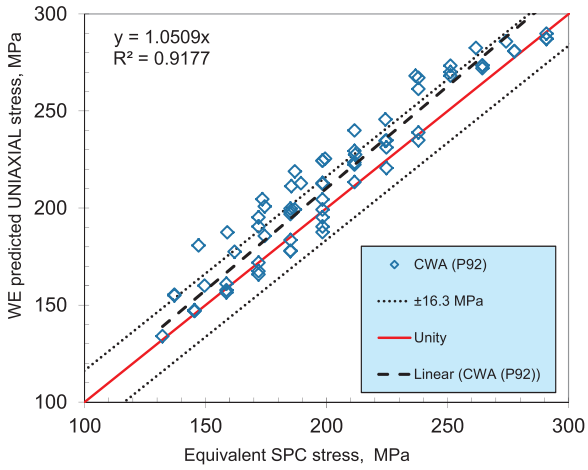

Fig. 11. CWA model calculated uniaxial creep stress against equivalent stress for P92 using the Wilshire model for uniaxial interpolation.

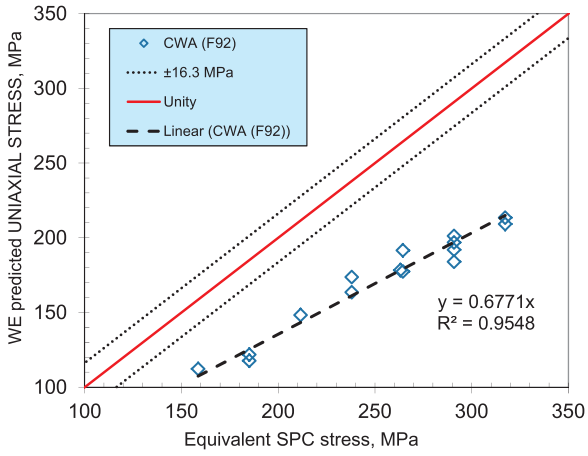

Fig. 12. CWA model calculated uniaxial creep stress against equivalent stress for F92 using the Wilshire model for uniaxial interpolation.

3.3.2. Empirical "force to stress conversion" method used in the draft standard

For the SP standard a fully empirical force to stress conversion model (EFS) was chosen by the TC101 work group as the preferred methodology for Annex G. The EFS described in Eq. (7) was optimized to all available uniaxial and SPC data. The acquired Ψ_{EFS} is dependent

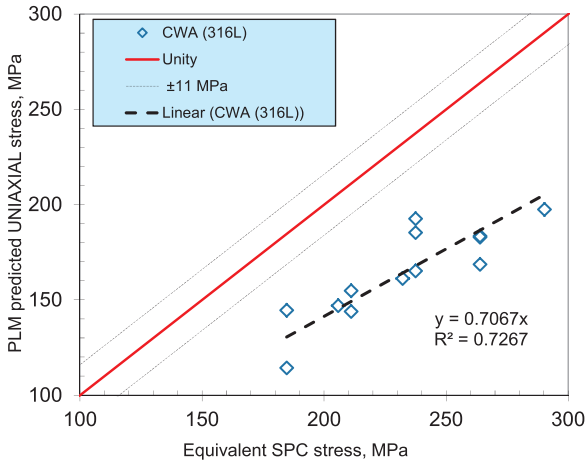

Fig. 13. CWA model calculated uniaxial creep stress against equivalent stress for 316 L using the Larson-Miller model for uniaxial interpolation.

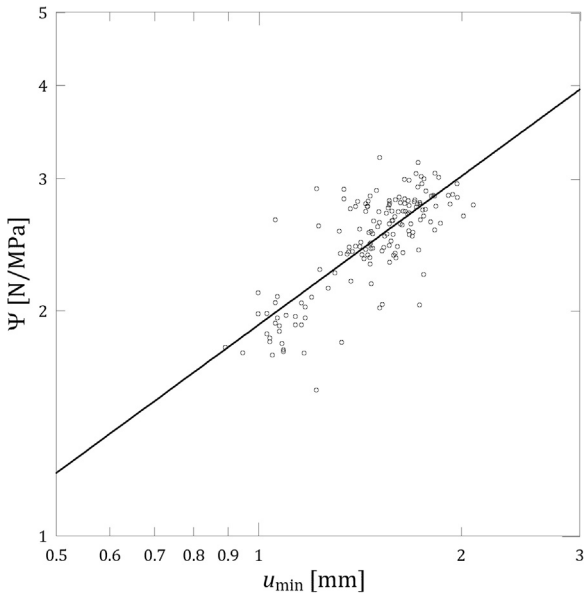

Fig. 14. Relationship between Ψ_{EFS} (PSI) and the deflection u_{min}.

on the measured deflection u_{min} at the location of the minimum deflection rate $\dot{u}_{min}$. It is to be emphasized that the given fitting parameters were optimized on a much larger data base than the round robin tests assessed here. In total, 119 uniaxial and 182 SPC data points were used for the fit. Also, it should be emphasized that the used data set mainly comprises of SPC data from low alloy and 9Cr steels, such as 14MoV63, X20CrMoV121, P91, P92 and Eurofer-97 but also includes the small data set of 316 L. The interpolated uniaxial stresses of specific test materials were calculated using isothermal log-linear fits of stress-time data and not using time-temperature parameters as in this paper. Note that this could potentially lead to some over prediction of uniaxial creep strength for short rupture times outside the uniaxial data range.

The EFS optimized force to stress ratio $\Psi_{EFS} = F/\sigma$ is:

$$\Psi_{EFS} = 1.9162 \cdot u_{min}^{0.6579}\,[\mathrm{N/MPa}] \tag{7}$$

The Ψ value as a function of deflection for the fully optimized data set shown in Fig. 14. It can be seen that the scatter in u_{min} can be substantial.

The equivalent SPC stress estimates using the EFS formulation are shown in relation to the uniaxial creep stress at the same rupture time in Figs. 15–17 for P92, F92 and 316 L respectively.

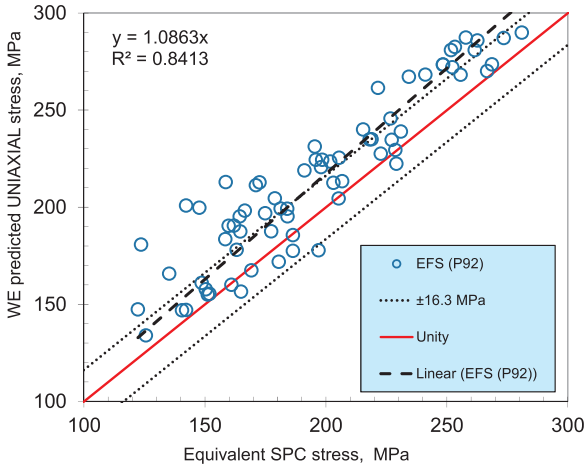

Fig. 15. EFS model calculated equivalent stress against uniaxial creep stress for P92 using the Wilshire model for uniaxial interpolation.

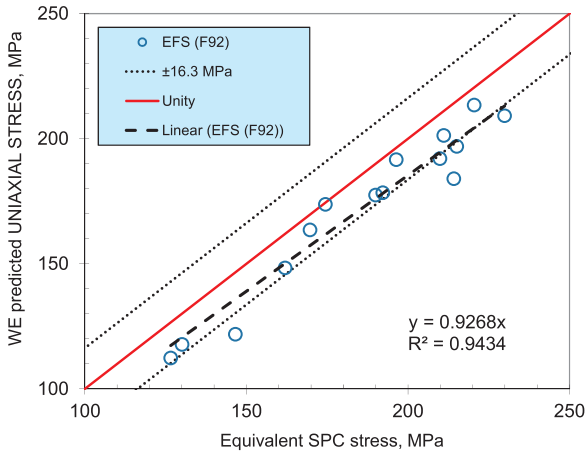

Fig. 16. EFS model calculated equivalent stress against uniaxial creep stress for F92 using the Wilshire model for uniaxial interpolation.

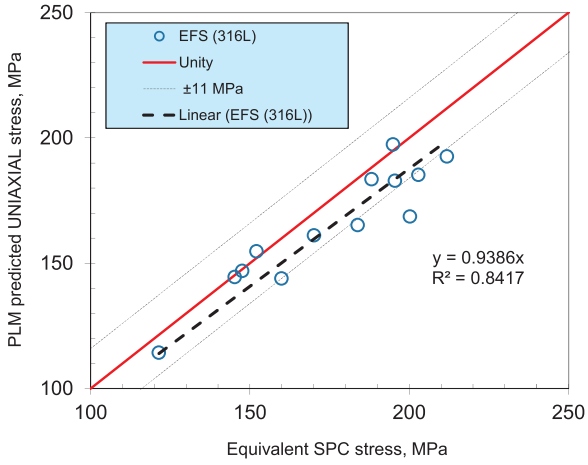

Fig. 17. EFS model calculated equivalent stress against uniaxial creep stress for 316 L using the Larson-Miller model for uniaxial interpolation.

For P92 it can be seen that the SPC estimates are well in line with the corresponding uniaxial test stresses, with the right gradient, although the strength is under predicted (~9%). This is likely to be caused by the shortened rupture lives from the detected premature cracking. It is also clear that the scatter has increased in comparison to the CWA fit.

For both F92 and 316 L the SPC equivalent stress estimates are also well in line with the uniaxial test stresses, though in these cases, the uniaxial stresses are somewhat over predicted (~7%). This is likely to be caused by the higher deflection at minimum deflection rate than what is seen for the main bulk of SPC data included in the fit of the model.

Annex G in the soon to be published standard also includes a formula for converting the measured minimum deflection rate to an equivalent minimum creep strain rate. The equivalent minimum strain rate $\dot{\varepsilon}_{\min}$ (1/h) can be calculated from the minimum deflection rate $\dot{u}$ (mm/h) of a SPC test as described in Eq. (8). The optimized parameters are from the same data pool as for the equivalent stress calculations.

$$\dot{\varepsilon}_{min} = 0.3922 \cdot \dot{u}_{\min}^{1.1907} (1/\mathrm{h}) \tag{8}$$

The correlation between minimum deflection rate and minimum uniaxial strain rate is shown in Fig. 18.

A comparison of the modelled SPC equivalent minimum creep strain rates and the Monkman-Grant defined uniaxial minimum strain rates

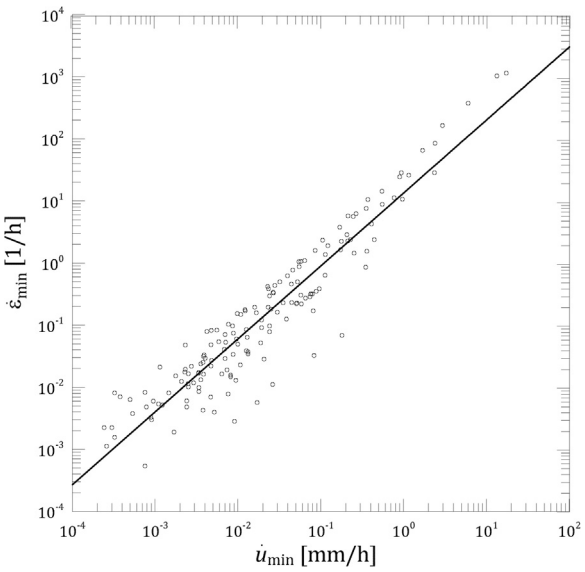

Fig. 18. Relation between the minimum deflection rate $\dot{u}_{\min}$ and the minimum strain rate $\dot{\varepsilon}$. Note that the presented data set includes data from more materials than the ones assessed in this paper.

(see Fig. 5) is shown for P92 and 316 data in Fig. 19a) and b). The F92 is not assessed due to the confidential nature of the uniaxial tests.

As can be seen, the equation for changing minimum deflection rate into minimum strain rate underestimates the uniaxial strain rate by a factor of about 2.5 for P92 and in the case of 316 L the strain rate is overestimated with about the same factor. The interesting aspect of this is that if the difference between materials is a factor of 5, the same as calculated for the Monkman-Grant in table Table 5.

3.3.3. Modified Chakrabarty SPC model

The third benchmarked model is the modified Chakrabarty model (MCH). The MCH is a full deflection range Ψ model that mimics the above given EFS model. The benefit of the MCH is the somewhat higher predicted Ψ values for high ductility materials and the possibility to account for different types of test set-ups. Note that the model's capability to work with other test set-ups has to date only been tested on the round robin data from Kagoshima (KAG). The KAG test set-up has a differing puncher diameter of 2.38 mm instead of 2.5 mm. The expected difference in test stresses and rupture times are small. In the near future, assessment of historical data with 2 mm balls will be conducted.

The analytical description of the MCH model is shown in Fig. 20 in relation to the classical $\Psi_{Cha}(u)$ Chakrabarty membrane stretch formulation and the EFS model. The Ψ_{MCH} is a linear function of deflection. The slope and intercept of the MCH line is solved from the $\Psi_{Cha}(u)$ by defining a test set-up dependent slope and a fixed point on the line. The linear function slope is acquired from the derivative $\delta\Psi_{Cha}/\delta u$ at 60% of the deflection u_m. u_m is the deflection where $\Psi_{Cha}(u)$ reaches its maximum value. For the standard test set-up u_m = 1.57 mm. The 60% was chosen to give $\Psi_{MCH} = \Psi_{EFS}$ at a deflection of about 1 mm. Note that the CWA model with k_{SP} = 1 was originally optimized for SPC data with $u_{\min}$ at about 1 mm. The intercept for the line can be calculated by applying the above defined slope through a specified fixed point. The chosen fix-point is also based on the $\Psi_{Cha}(u)$, i.e. $\Psi_{MCH}(u_m) = (1 + h_0/r)\cdot\Psi_{Cha}(u_m)$. This point is a best estimate of the ultimate tensile strength for ductile materials by classical SP tests [11,23].

The MCH optimized force to stress ratio for the standard test set-up $\Psi_{MCH} = F/\sigma$ is:

$$\Psi_{MCH} = 0.6143 + 1.2954 \cdot u_{\min}\,[\mathrm{N/MPa}] \tag{9}$$

The MCH model predictions are shown in relation to the uniaxial creep stresses at the same rupture time in Figs. 21–23 for P92, F92 and

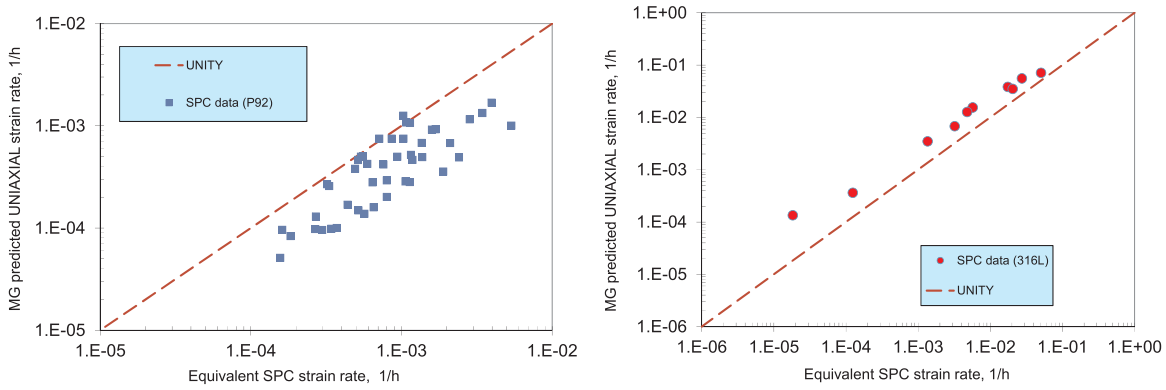

Fig. 19. Monkman-Grant predicted uniaxial minimum strain rate (at measured SPC rupture time) plotted against calculated SPC equivalent minimum strain rate for a) P92 and b) 316 L.

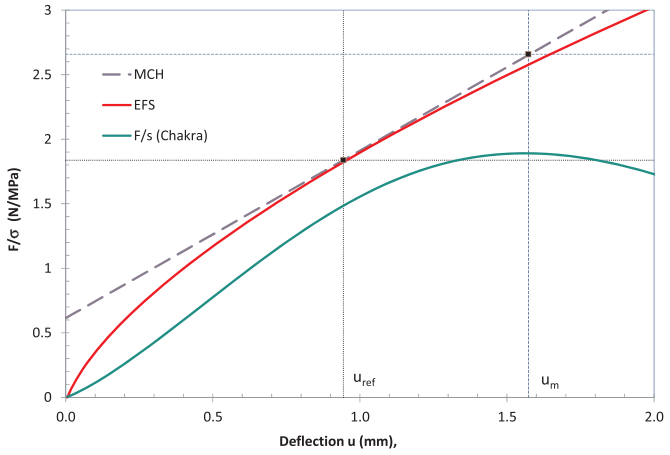

Fig. 20. Definition of the linear model Ψ_{MCH} from Ψ_{EFS} and $\Psi_{Cha.}$, $u_{ref} = 0.6 \cdot u_{max}$.

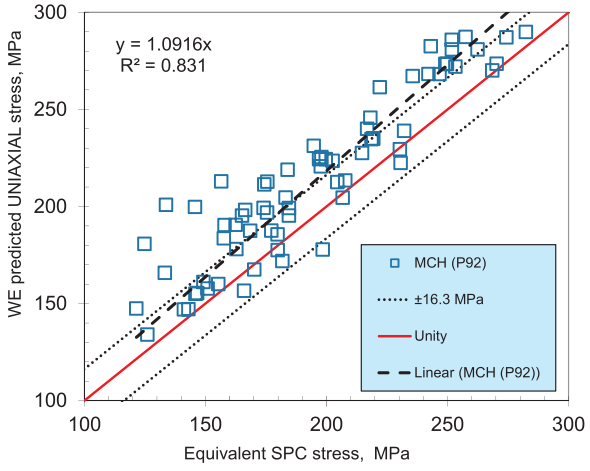

Fig. 21. MCH model calculated equivalent stress against uniaxial creep stress for P92 using the Wilshire model for uniaxial interpolation.

316 L respectively. The MCH scatter for the P92 is, as it was for the EFS model, larger than the CWA and about the same as for the EFS model. This is to be expected since the MCH was defined to mimic the ESF at $u = 1$ mm. In the case of F92 and 316 L the MCH model predictions give slightly improved creep strength estimates in comparison to the EFS.

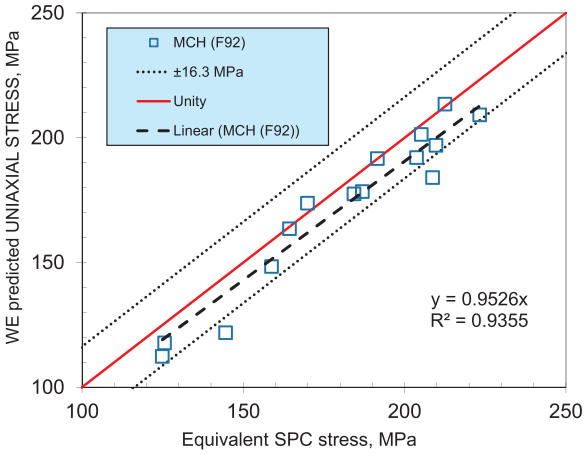

Fig. 22. MCH model calculated equivalent stress against uniaxial creep stress for F92 using the Wilshire model for uniaxial interpolation.

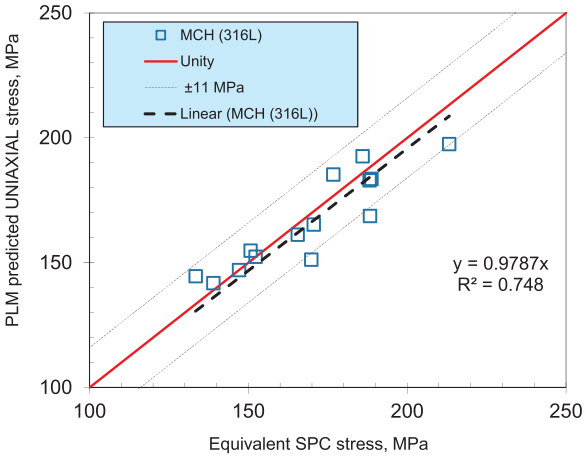

Fig. 23. MCH model calculated equivalent stress against uniaxial creep stress for 316 L using the Larson-Miller model for uniaxial interpolation.

4. Discussion

The SPC assessments of the TC-101 RR test data show that the new models that include deflection dependency in the force to stress conversion clearly improve the accuracy of the estimated equivalent SPC stress for different types of steels. However, it is also clear that inherent

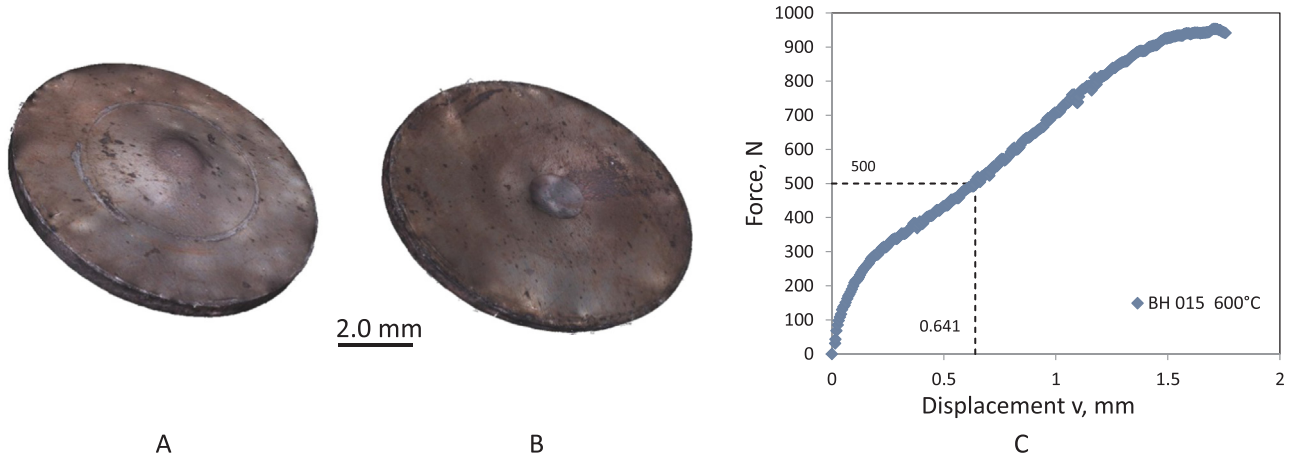

Fig. 24. a) Top and b) bottom side of a small punch creep specimen interrupted after loading with 500 N at 600 °C and c) a classical SP constant deflection rate test at the same temperature.

scatter in the measured deflection at minimum deflection rate can cause rather large errors in the calculated equivalent stress. For example, the P92 tests conducted at 625 °C and 350 N by three different laboratories measured the deflection at minimum deflection rate to be 0.61, 1.07 and 1.38 mm. The measured time to rupture was very stable at 194 h ± 10 h for the tests in question. The equivalent stress calculated for the largest deflection was 27% smaller than the uniaxial stress for the specific test rupture time. The smallest deflection again gave a 24% larger estimate. This emphasizes the importance of measuring the total deflection correctly in SPC testing. In this case the low ductility of the P92 material could be the culprit causing the scatter, but differences in the deflection measurement system, calibrations and test start-up procedure will most certainly also cause scatter.

Since the equivalent stress calculation is dependent on robust determination of the location of the minimum deflection rate it would clearly also be of importance to define a robust methodology to retrieve it. The successful differentiation of the time-strain curve in standard uniaxial tests and the time-deflection curve in a SPC test is somewhat sensitive to data acquisition sampling rate, LVDT noise and the adopted data smoothing method. As most raw data assessors know, the calculated rates over a specified amount of data points (or over a specified time Δt) will not necessarily be smooth. A potential simplification in the "SPC to uniaxial" conversion could be to use ½ life values instead of finding the minimum through differentiation, i.e. using deflection at ½ life ($½{\cdot}t_r$) for equivalent stress calculation and use the deflection at three points, e.g. deflection at 1/3, half and 2/3 of life to determine the test specific deflection rate. This approach will be tested in future work.

Another way of improving the equivalent stress estimates when the measured u_{min} are scattered is to conduct some constant displacement rate small punch tests (SP) at the specific creep temperatures. These tests will give good reference in expected initial deflection at loading. The measured SP test deflection (at specified SPC load) can then be used as an "after loading" value to which the SPC creep deflection is added. A typical constant deflection rate SP test is shown in Fig. 24 together with an interrupted SP test piece. The measured permanent displacement of the SP sample (0.604 mm) is well in line with what the reading acquired from the SP displacement curve at 500 N (0.641 mm).

Finally, we note the importance of performing repeated tests. SPC tests are usually rather short in duration and the creep property estimates would most likely improve by using test condition specific averages of deflection and rupture time instead of test by test values.

When the relationship between uniaxial minimum creep rates and SPC minimum deflection rates were analysed it was noticed that the SPC minimum deflection rates seemed to be a better descriptor of time to rupture ($1/t_r$) than the material specific uniaxial minimum strain rates. This could call for an additional correction factor for materials

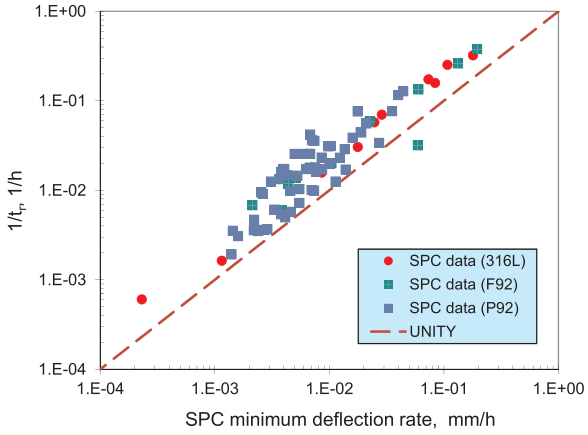

Fig. 25. Measured SPC minimum deflection rates against measured $1/t_r$ for P92, F92 and 316 L.

with clearly different Monkman-Grant exponents to acquire the uniaxial minimum strain rate. The measured minimum deflection rates plotted against the measured inverted time to rupture values are shown for all three round robin materials in Fig. 25.

As a consequence, it could be postulated that a "SPC-Monkman-Grant" (SMG) empirical approach, giving the correlation between the measured deflection rate and the measured t_r, is seemingly insensitive to the material and could be applied on all the round robin materials as;

$$t_r = \frac{D}{\dot{u}^n}(\mathrm{h}) \tag{10}$$

where $D = 0.521$ and $n = 0.959$ are material independent constants.

With a testing standard in place and with robust and accurate models for determining both uniaxial creep strength and minimum strain rate looking to be established, the attractiveness of the SPC testing is clearly increased. SPC material property determination from scoop samples extracted from in-service components could become an important tool for validation of "fit for service" materials in high temperature industrial applications. Thus, the SPC can become an accepted "standard" route for life extension decision making.

5. Conclusions

In this paper three assessment methodologies for determining equivalent stresses from SPC tests have been compared for three different steels. The method to estimate the uniaxial minimum strain rate from SPC data is also included in the forthcoming international standard and

has been applied on the ECISS TC101 WG1 round robin SPC data.

The following conclusions can be drawn from these assessments on P92, F92 and 316 L steels;

1. The two analysed force to stress conversion models that include deflection as a dependent variable are superior to the classical CWA model with a constant conversion factor.
2. The scatter in the calculated equivalent stress values is mainly caused by uncertainties in the determination of the deflection u where the minimum deflection rate is reached and by premature cracking.
3. The tested P92 steel has ductility issues and shows premature cracking mainly in the 600 °C and 625 °C SPC tests.
4. The (uniaxial) creep strength of the more ductile materials 316 L and F92 are estimated well by the calculated equivalent SPC stresses using the EFS model proposed for the new standard.
5. When converting SPC minimum deflection rates to uniaxial minimum strain rates a further correction might have to be considered to account for differences in the uniaxial Monkman-Grant parameters.
6. The correlation between minimum deflection rate and the inversed time to rupture in SPC tests seems to be material independent.
7. The new standard will clearly improve the attractiveness of the SPC test in general and is likely to improve the applicability of the testing technique for industrial applications.

Acknowledgments

The support of all the laboratories involved in the ECISS TC101 WG1 and ECCC small punch creep round robins is gratefully acknowledged.

Data availability

The P92 RR data can be made available on request from each testing laboratory separately. It is foreseen that the full set of data will become available in the European Commission data base MATDB (https://odin.jrc.ec.europa.eu/odin/index.jsp) in the near future.

References

[1] CEN Workshop Agreement CWA 15267, European Code of Practise: Small Punch Test Method for Metallic Materials., 2007.
[2] S. Komazaki, T. Kato, Y. Kohno, H. Tanigawa, Creep property measurements of welded joint of reduced-activation ferritic steelby the small-punch creep test, Mater. Sci. Eng. A 510–511 (2009) 229–233.
[3] B. Gülçimen, P. Hähner, Determination of creep properties of a P91 weldment by small punch testing and a new evaluation approach, Mater. Sci. Eng. A 588 (2013) 125–131.
[4] L. Zhao, H. Jing, L. Xu, Y. Han, J. Xiu, Y. Qiao, Evaluating of creep property of distinct zones in P92 steel welded joint by small punch creep test, Mater. Des. 47 (2013) 677–686.
[5] B. Ule, T. Sustar, F. Dobes, K. Milicka, V. Bicego, S. Tettamanti, K. Maile, C. Schwarzkopf, M.P. Whelan, R.H. Kozlowski, J. Klaput, Small punch test method assessment for the determination of the residual creep life of service exposed components: outcomes from a interlaboratory exercise, Nucl. Eng. Des. 192 (1999) 1–11.
[6] R.J. Lancaster, W.J. Harrison, G. Norton, An analysis of small punch creep behaviour in the γ titanium aluminide Ti–45Al–2Mn–2Nb, Mater. Sci. Eng. A 626 (2015) 263–274.
[7] J.P. Rouse, F. Cortellino, W. Sun, T.H. Hyde, J. Shingledecker, Small punch creep testing: review on modelling and data interpretation, Mater. Sci. Technol. 29 (11) (2013) 1328–1345.
[8] E. Altstadt, H.E. Ge, V. Kuksenko, M. Serrano, M. Houska, M. Lasan, M. Bruchhausen, J.-M. Lapetite, Y. Dai, Critical evaluation of the small punch test as a screening procedure for mechanical properties, J. Nucl. Mater. (2015).
[9] M. Bruchhausen, T. Austin, S. Holmström, E. Altstadt, P. Dymacek, S. Jeffs, R. Lancaster, R. Lacalle, K. Matocha, European standard on small punch testing of metallic materials. Proceedings of the ASME 2017 Pressure Vessels and Piping Conference, PVP2017 July 16-20, 2017, Waikoloa, Hawaii, USA, 2017.
[10] S. Holmström, P. Dymacek, S.P. Jeffs, R.J. Lancaster, R.C. Hurst, A. Tonti, E. Poggio, E. Vacchieri, Small punch creep testing of P92 steel and weld for inter-laboratory comparison and standardization, ECCC Creep and Fracture Conference 2017, ISBN 978-3-514-00832-8, Steel Institute VDEh, 2017.
[11] S. Holmström, P.Hähner, R.C. Hurst, M. Bruchhausen, B. Fischer, J-M Lapetite, M. Gupta, Small punch creep testing for material characterization and life time prediction, Proc. of the 10th Conference on Materials for Advanced Power Engineering, Liege, 2014. ISSN 1866-1793, pp. 627–635.
[12] D. Andrés, R. Lacalle, J.A. Álvarez, Creep property evaluation of light alloys by means of the Small Punch test: creep master curves, Mater. Des. 96 (2016) 122–130.
[13] S. Komazaki Naveena, Evaluation of creep rupture strength of high nitrogen ferritic heat-resistant steels using small punch creep testing technique, Mater. Sci. Eng. A 676 (2016) 100–108.
[14] S.P. Jeffs, R.J. Lancaster, T.E. Garcia, Creep lifing methodologies applied to a single crystal superalloy by use of small scale test techniques, Mater. Sci. Eng. A 636 (2015) 529–535.
[15] F. Dobeš, P. Dymáček, Fracture-based correlation of uniaxial and small punch creep data, Theor. Appl. Fract. Mech. 86 (2016) 34–38.
[16] B. Wilshire, P.J. Scharning, Long-term creep life prediction for a high chromium steel, Scr. Mater. 56 (8) (. 2007) 701–704.
[17] F.R. Larson, J. Miller, Trans. ASME 74 (1952) 765–771.
[18] S. Holdsworth, (Ed.), ECCC Recommendations - Volume 5 Part Ic [Issue 2], Recommendations and Guidance for the assessment of full size stress relaxation data sets, 2003.
[19] S. Holmström: MatDB catalog of uniaxial tensile test data for P92 steel, version 1.0, European Commission JRC, [Catalog], 2018. ⟨http://dx.doi.org/10.5290/41⟩.
[20] M. Schirra, Creep rupture strength and creep tests on the EFR structural material 316L(N), DIN 1.4909, Nucl. Eng. Des. 147 (1) (1994) 63–78.
[21] F.C. Monkman, N.J. Grant, An empirical Relationship between rupture life and minimum creep rate in creep-rupture tests, Proc. ASTM Int. 56 (1956) 593–620.
[22] J. Chakrabarty, theory of stretch forming over hemispherical punch heads, Int. J. Mech. Sci. 12 (4) (1970) 315–325.
[23] S. Holmström, et al., Determination of High Temperature Material Properties of 15-15Ti Steel by Small Specimen Techniques, Publications Office of the European Union, Luxembourg, 2017, http://dx.doi.org/10.2760/259065 EUR 28746 EN.